

# Nanosize hexagonal tungsten oxide for gas sensing applications

Csaba Balázsi<sup>a,\*</sup>, Lisheng Wang<sup>b</sup>, Esra Ozkan Zayim<sup>c</sup>, Imre Miklós Szilágyi<sup>d</sup>,  
Katarína Sedlacková<sup>e</sup>, Judit Pfeifer<sup>a</sup>, Attila L. Tóth<sup>a</sup>, Pelagia-Irene Gouma<sup>b</sup>

<sup>a</sup> *Ceramics and Composites Laboratory, Research Institute for Technical Physics and Materials Science, Hungarian Academy of Sciences, Konkoly-Thege út 29-33, H-1121 Budapest XII., Hungary*

<sup>b</sup> *Department of Materials Science and Engineering, 314 Old Engineering Building, SUNY, Stony Brook, NY 11794-2275, USA*

<sup>c</sup> *Department of Physics, Faculty of Science and Letters, Istanbul Technical University, Maslak, Istanbul 80626, Turkey*

<sup>d</sup> *Department of Inorganic and Analytical Chemistry, Budapest University of Technology and Economics, H-1111 Budapest, Szt. Gellért tér 4, Hungary*

<sup>e</sup> *Thin Film Physics Laboratory, Research Institute for Technical Physics and Materials Science, Hungarian Academy of Sciences, Konkoly-Thege út 29-33, H-1121 Budapest, Hungary*

Available online 10 October 2007

## Abstract

Tungsten oxides and tungsten oxide hydrates are among the most used materials in electro-, photo- and gaso-chromic applications. Lately, tungsten oxides have been commonly applied as sensing layers for hazardous gas detection as well. In this work, a soft chemical nanocrystalline processing route has been demonstrated for the preparation of hexagonal tungsten oxides. The acidic precipitation was followed by hydrothermal and heat treatments at low temperatures. The morphology of parent phases, such as amorphous  $\text{WO}_3 \cdot 2\text{H}_2\text{O}$ , orthorhombic  $\text{WO}_3 \cdot 1/3\text{H}_2\text{O}$ , and resulting oxides with open structured nanosized hexagonal platelets of h- $\text{WO}_3$  particles have been studied by scanning electron microscopy (SEM), by conventional transmission electron microscopy (TEM) and by high resolution transmission electron microscopy (HRTEM). Structural and electrochemical performance of thin films have been determined by atomic force microscopy and cyclic voltammetry. The ion insertion properties of tungsten oxide hydrate and tungsten oxide films show a clear dependence on the presence of structural water and on the close packed structure. Sensing properties of the prepared tungsten oxides have been tested with respect to ammonia gas.

© 2007 Elsevier Ltd. All rights reserved.

**Keywords:** Soft chemical synthesis; Transition metal oxides; Nanocomposites; Sensors; Functional application

## 1. Introduction

Metal oxides are polymorphic compounds and controlled chemical processing may stabilize oxide polymorphs that would otherwise be energetically unstable. Recent studies by the authors' group<sup>1–3</sup> led to the hypothesis that the ability for selective detection of a particular gaseous analyte in the presence of interfering gas mixtures (i.e. sensor selectivity) is largely determined by the chosen crystalline polymorph (specific crystallographic phase) of a stoichiometric and pure metal oxide used for sensing. Transition metal oxide such as  $\text{MoO}_3$  and  $\text{WO}_3$  were

used as model systems in those studies. Orthorhombic ( $\alpha$ -phase)  $\text{MoO}_3$  was found to exhibit high specificity to the detection of ammonia and amines. Issues of structural stability due to the high volatility of this material, however, limit its use in high-temperature sensing applications. The search for alternative materials that are isostructural with  $\text{MoO}_3$  identified tungsten oxides as promising candidates. It seems that “loosely-bound” open structures are necessary in order to achieve selective amine detection, as they enable the reaction of lattice oxygen with the gas and provide easy mechanisms for accommodating the off-stoichiometric metal: O ratio. The layered structure tungsten oxide dihydrate ( $\text{H}_2\text{WO}_4 \cdot \text{H}_2\text{O}$ ) and the open structure hexagonal form of  $\text{WO}_3$  seem to be good candidates for the use of reaction-based, and adsorption (chemisorption)-based sensing applications. Several decades earlier  $\text{H}_2\text{WO}_4 \cdot \text{H}_2\text{O}$  was successfully applied as the parent phase for metastable hexagonal tungsten oxide representing an optimal substance in intercalation chemistry. For the preparation of  $\text{H}_2\text{WO}_4 \cdot \text{H}_2\text{O}$ , two main routes<sup>4,5</sup> are known. The main difference between these two

\* Corresponding author at: Ceramics and Composites Laboratory, Hungarian Academy of Sciences, Research Institute for Technical Physics and Materials Science, H-1525 Budapest, P.O. Box 49, Hungary. Tel.: +36 1 392 2249; fax: +36 1 392 2226.

E-mail address: [balazsi@mfa.kfki.hu](mailto:balazsi@mfa.kfki.hu) (C. Balázsi).

URLs: <http://www.mfa.kfki.hu/> (C. Balázsi),  
<http://www.mfa.kfki.hu/nanodp/ceramic/> (C. Balázsi).

methods is in the rate of precipitation caused by differing pH in the reaction solutions. The morphology and structural stability of precipitated grains is directly controlled by precipitation and precipitate washing conditions.<sup>6–9</sup> In the present study acidic precipitation is carried out by a nanocrystalline processing route; the preparation of nanocrystalline hexagonal  $\text{WO}_3$  is demonstrated in a powder bed and in a thin layer over a silicon wafer deposited from a precursor suspension in situ with the purpose to integrate sensing layers into silicon chip technology. Electrochemical and sensing properties of the prepared tungsten oxides are tested under normal testing conditions.

## 2. Experimental details

### 2.1. Sample preparation

$\text{H}_2\text{WO}_4 \cdot \text{H}_2\text{O}$  samples were prepared by acidic precipitation<sup>4–6</sup> from sodium tungstate solution. The preparation method of Zocher combining washing and centrifuging the precipitated gel was modified.<sup>10</sup> An overnight cooling of the freshly precipitated gel was applied before washing of the gel. The resulted gels were washed and centrifuged 3–5 times depending on the process. Suspensions of the washed gels were passed to hydrothermal dehydration. The hydrothermal reaction was carried out in Parr acid digestion bombs at autogenous pressure at  $125 \pm 5^\circ\text{C}$ . Products after hydrothermal dehydration were dried at room temperature or used as received suspensions. Droplet(s) of the as received suspension were deposited onto ITO conductive transparent glass and (110) oriented silicon wafers. The silicon wafer covered with the deposit and the resulted powder was then passed to final dehydration ( $330\text{--}340^\circ\text{C}$  furnace temperature, 90 min annealing time, ambient air).

### 2.2. Measurements

Structural characterization was conducted using X-ray diffraction (Bruker AXS D8 Discover X-ray diffractometer with  $\text{Cu K}\alpha$  radiation) and in situ high-temperature X-ray diffraction (HT-XRD), PANalytical X'pert Pro MPD X-ray diffractometer equipped with an Anton Paar HTK-2000 high-temperature XRD camera using  $\text{Cu K}\alpha$  radiation. HT-XRD experiments were performed in static air using a  $10^\circ\text{C min}^{-1}$  heating rate between XRD measurements.

The morphology of the samples was studied by scanning electron microscopy (LEO 1540XB field emission SEM). The structure of samples was investigated further by conventional transmission electron microscopy (TEM) using a Philips CM-20 microscope and by high-resolution transmission electron microscopy (HRTEM) with a JEOL 3010 microscope. AFM measurements of  $\text{WO}_3 \cdot 1/3\text{H}_2\text{O}$  layers deposited onto  $5 \mu\text{m} \times 5 \mu\text{m}$  Corning glass (2947) substrates were also carried out.

Electrochemical properties of tungsten oxide hydrate thin films were studied by cyclic voltammetry.<sup>11</sup> The  $\text{WO}_3 \cdot 1/3\text{H}_2\text{O}$  films were prepared directly from suspensions (received from the hydrothermal process) on ITO conductive transparent glass

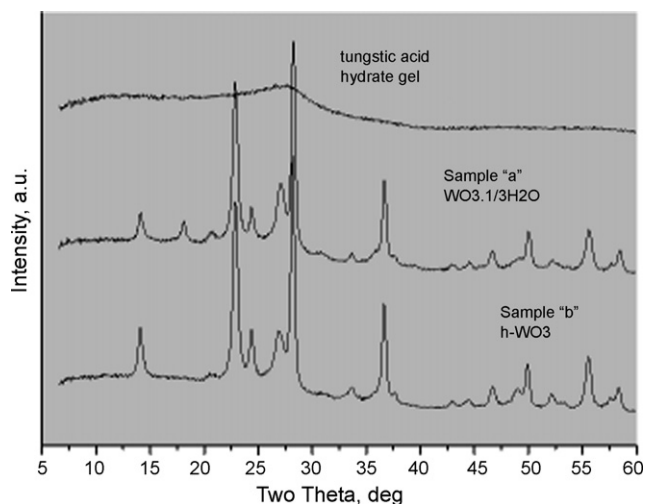


Fig. 1. XRD patterns of Zocher type tungstic acid hydrate gel and its dehydration derivatives. Sample "a" identified as  $\text{WO}_3 \cdot 1/3\text{H}_2\text{O}$  (JCPDS card 35–270) and sample "b" identified as h- $\text{WO}_3$  (JCPDS card 33–1387).

substrates. The substrates were consecutively rinsed with acetone, methanol and isopropyl alcohol and dried in air. The spin coating speed was set at 2000 rpm.

Sensing layers have been produced by spin coating 10 mg powder/5 ml *n*-butanol suspensions on  $\text{Al}_2\text{O}_3$  substrates with Au-metallization. Sensing tests were carried out in the gas flow bench set-up at SUNY, Stony Brook.<sup>12</sup> The gases used in the sensing setup were UHP nitrogen (Praxair), UHP oxygen (Praxair), 1000 ppm ammonia in nitrogen (BOC gases). Concentration of ammonia was varied by varying its flow rate in conjunction with nitrogen flow rates. The gases were controlled through 1479 MKS Mass flow controllers whose channels were connected to a Type 247-MKS 4-channel readout which is calibrated to read the flow rate of the gases directly in sccm. The combined flow rate of the gases was maintained at 1000 sccm. The gas mixture is passed through a tube furnace (Lindberg/Blue), which

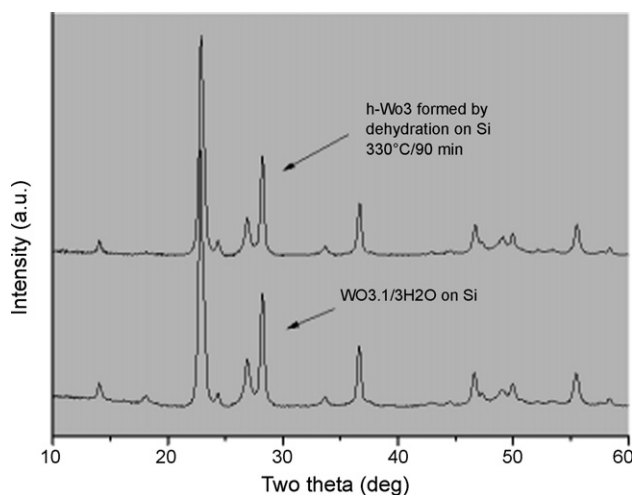


Fig. 2. XRD patterns of tungsten oxide layers deposited on 100 Si wafer. Sample " $\text{WO}_3 \cdot 1/3\text{H}_2\text{O}$ " (JCPDS card 35–270) was formed by depositing a droplet of suspension on Si and then dried at RT, under air. Sample "h- $\text{WO}_3$ " (JCPDS card 33–1387), the preceding sample heat-treated at  $330^\circ/90$  min, under air.

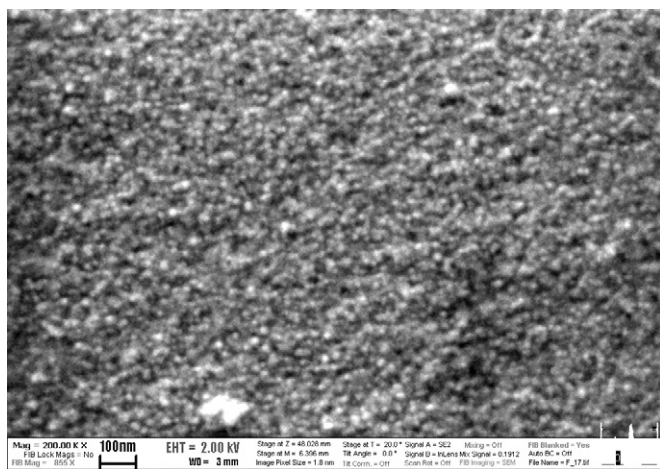


Fig. 3. Tungstic acid hydrate mother phase gel precipitated according to the modified Zocher process.

can be heated at a programmed rate. The sensing element is placed inside the tube furnace with quartz tube (2.5 cm diameter, 60 cm length) and is electrically connected to outside leads using gold wires. Sensing experiments were carried out at room temperature and at various temperatures up to 300 °C. Electrical resistance measurements<sup>1,2</sup> of the sensing films as a function of the gas concentration were carried out using an Agilent 34401 digital multimeter.

### 3. Results

Figs. 1 and 2 show XRD patterns of the samples derived from the Zocher type tungstic acid gel. Sample “1a” is the powder product after hydrothermal dehydration and sample “1b” is the powder product after dehydration under air of sample “a”. XRD patterns were compared and checked with the Joint Committee on Powder Diffraction Standards files. Sample “1a” was identified as  $\text{WO}_3 \cdot 1/3\text{H}_2\text{O}$  (JCPDS card 35–270) and sample “1b” was identified as  $\text{h-WO}_3$  (JCPDS card 33–1387). Simi-

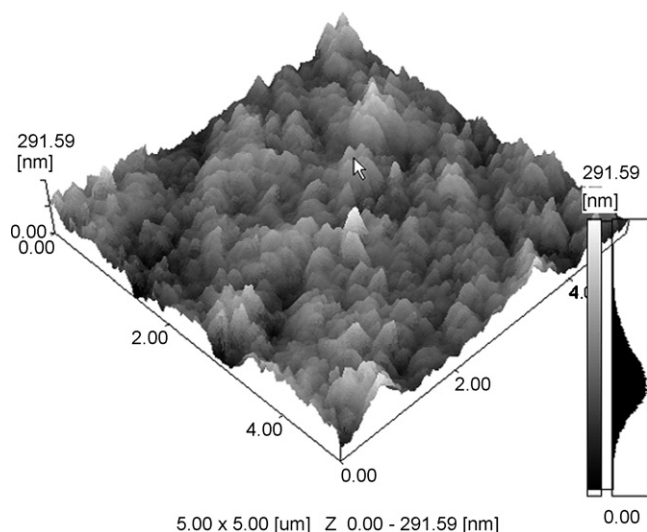


Fig. 4. AFM images of  $\text{WO}_3 \cdot 1/3\text{H}_2\text{O}$  nanocrystalline film after two washing processes.

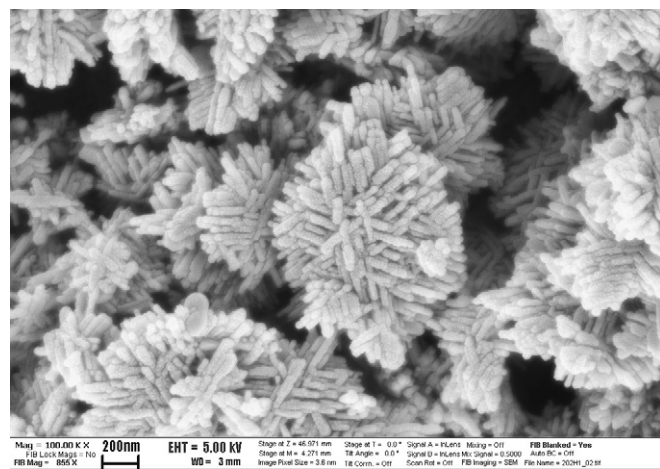


Fig. 5. SEM image of  $\text{h-WO}_3$  derivative gained from the precursor shown in Fig. 3.

larly Zocher type tungstic acid derivatives deposited on (100) Si wafer are shown in Fig. 2. The sample “ $\text{WO}_3 \cdot 1/3\text{H}_2\text{O}$ ” is formed by drying (room temperature, under air) a droplet of suspension on the Si wafer; sample “ $\text{h-WO}_3$ ” is the dehydration product of sample “ $\text{WO}_3 \cdot 1/3\text{H}_2\text{O}$ ” at 330°/90 min under air. Comparing the patterns it is clear, that the dehydration process of  $\text{WO}_3 \cdot 1/3\text{H}_2\text{O}$  to  $\text{h-WO}_3$  is undisturbed even in layers on top of Si wafer.

In Fig. 3 tungstic acid hydrate gel, the mother phase of the nanosize dimension derivatives applied for sensing layers is shown. This morphology seems to be promising as a precursor for sensing layers with nanosize dimension grains. AFM images in Fig. 4 show  $\text{WO}_3 \cdot 1/3\text{H}_2\text{O}$  films derived from the mother phase shown in Fig. 3. The grain size is uniform with grains packed together to form a nanocrystalline film.

Fig. 5 shows hexagonal  $\text{WO}_3$  prepared by hydrothermal and air ambient dehydration processes from the mother phase. The crystalline derivative consists of aggregates (1–2  $\mu\text{m}$ ) of rods and platelets with thickness of ~20–30 nm.

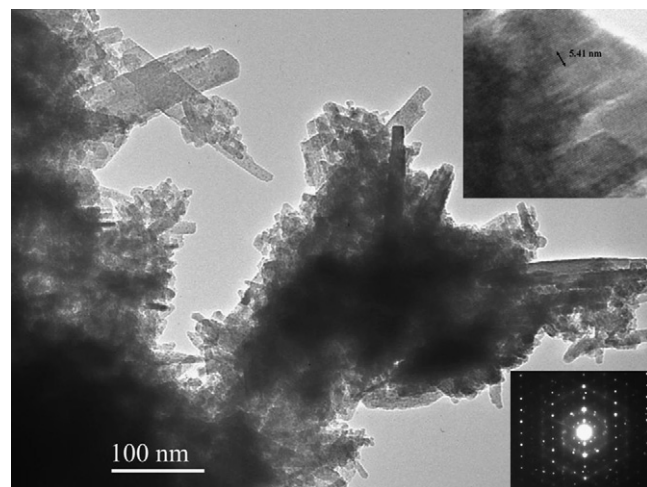


Fig. 6. Plan view TEM image of  $\text{WO}_3 \cdot 1/3\text{H}_2\text{O}$  film.



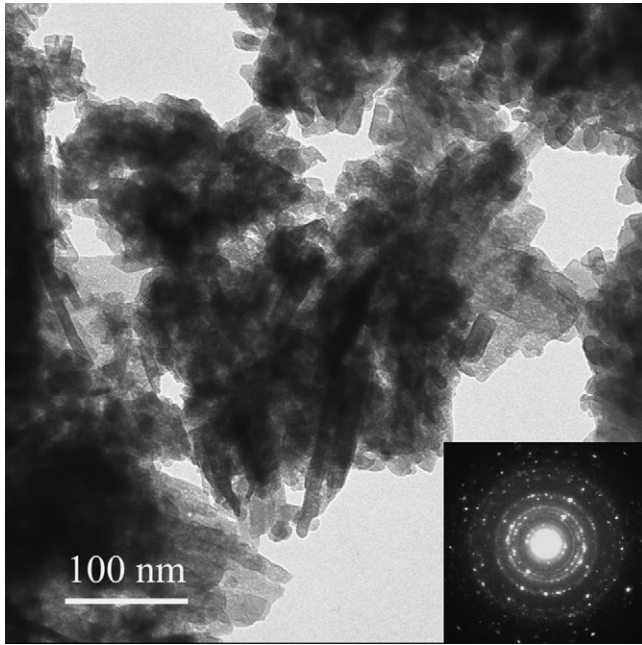


Fig. 7. Plan view TEM image of h-WO<sub>3</sub> film after annealing.

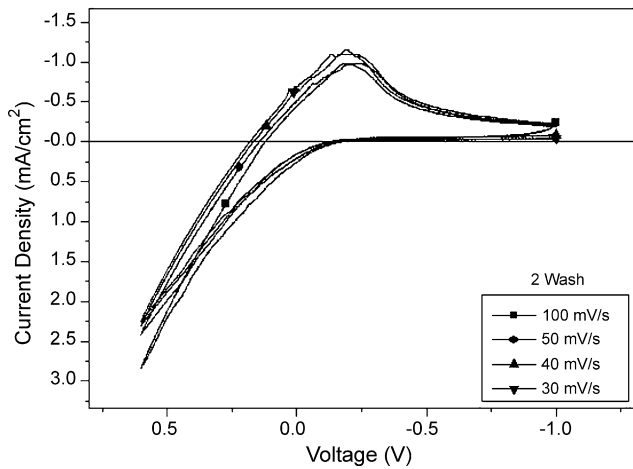


Fig. 8. Cyclic voltammetry of WO<sub>3</sub>·1/3H<sub>2</sub>O film derived from a 2× washed precursor gel with respect to various scan rates, in 1 M LiClO<sub>4</sub>/PC.

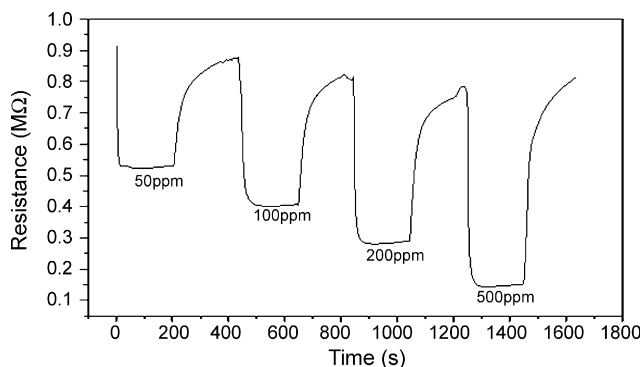


Fig. 9. Sensing responses of h-WO<sub>3</sub> to various levels of NH<sub>3</sub> doses at 300 °C.

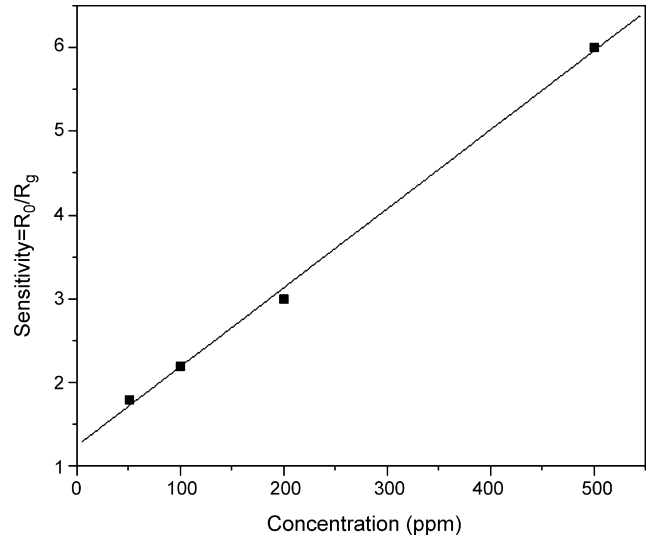


Fig. 10. Sensitivity of h-WO<sub>3</sub> sensor to NH<sub>3</sub> as a function of concentration.

Carrying out TEM and HRTEM investigations (see Figs. 6 and 7) we found the correlation between structure and other properties of WO<sub>3</sub> films. The average size of crystallites after hydrothermal treatment is ~50–100 nm and the electron diffraction showed the orthorhombic phase of WO<sub>3</sub>·1/3H<sub>2</sub>O crystallites. After 330 °C air ambient treatment of the powder, the average size of WO<sub>3</sub> crystallites decreased to ~30–50 nm. Electron diffraction confirmed the phase change from orthorhombic to hexagonal one.

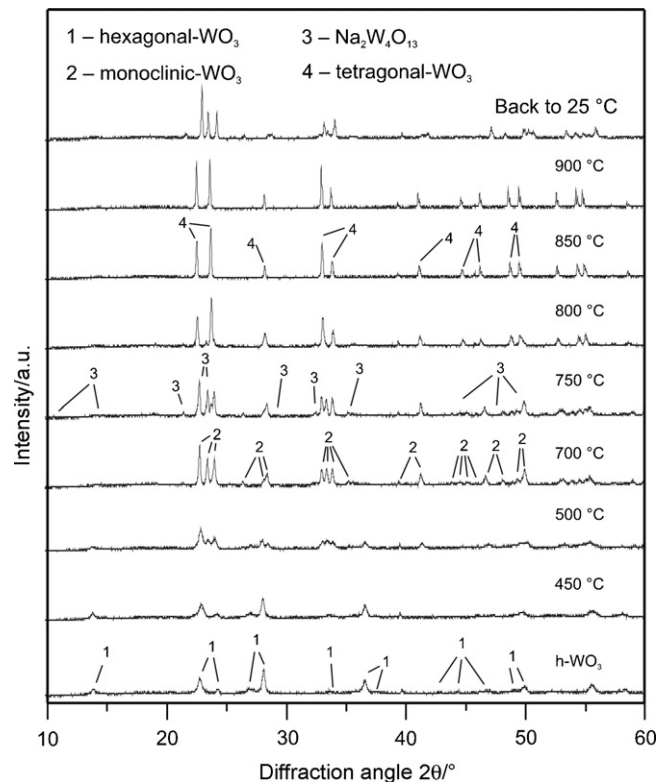


Fig. 11. In situ HT-XRD patterns of h-WO<sub>3</sub> in static air.

Cyclic voltammograms of samples with crystalline  $\text{WO}_3 \cdot 1/3\text{H}_2\text{O}$  films derived from a  $2\times$  washed precursor gel are given in Fig. 8. While no anodic peaks are observed, there is a well-defined cathodic peak, indicating the quick process for lithium insertion, even at very low voltages.

The plots in Fig. 9 show the response of the sensing layer prepared from h- $\text{WO}_3$  to ammonia at various levels of ammonia in one dose. The measurement was carried out at  $300^\circ\text{C}$ . The films showed a decrease in resistance on exposure to  $\text{NH}_3$ , which is characteristic to an  $n$ -type semiconductor. The layers were found to be sensitive in the concentration range of 50–500 ppm and the sensing response was found to change linearly with ammonia concentration (Fig. 10). The sensitivity at lower temperature was not satisfactory; the sensitivity at higher temperature seems to be promising. In situ HT-XRD patterns of h- $\text{WO}_3$  in static air (Fig. 11) showed that h- $\text{WO}_3$  was stable up to  $425^\circ\text{C}$ .

#### 4. Conclusion

In this paper we report on the acidic precipitation route for preparation of nanosize  $\text{WO}_3 \cdot 1/3\text{H}_2\text{O}$  and h- $\text{WO}_3$  powders and suspensions. The electrochemical and gas sensing properties of layers based of nanopowders have been studied. The layers were electrochemically active and sensitive to  $\text{NH}_3$ .

#### Acknowledgements

The work was supported by the bilateral NSF-OTKA-MTA co-operation, contract no. MTA:96 OTKA: 049953 and also by a GVOP-3.2.1.-2004-04-0224/3.0 grant.

#### References

1. Prasad, A. K., Kubinski, D. and Gouma, P. I., Comparison of sol-gel and RF sputtered  $\text{MoO}_3$  thin film gas sensors for selective ammonia detection. *Sens. Actuators*, 2003, **B9**, 25–30.
2. Prasad, A. K., Gouma, P. I., Kubinski, D. J., Visser, J. H., Soltis, R. E. and Schmitz, P. J., Reactively sputtered  $\text{MoO}_3$  films for ammonia sensing. *Thin Solid Films*, 2003, **436**, 46–51.
3. Gouma, P. I., Nanostructured polymorphic oxides for advanced chemosensors. *Rev. Adv. Mater. Sci.*, 2003, **5**, 123–138.
4. Zocher, H. and Jacobson, K., Über Taktosole. *Kolloidchem. Beih.*, 1929, **28**, 167–205.
5. Freedman, M. L., The tungstic acids. *J. Am. Chem. Soc.*, 1959, **81**, 3834–3839.
6. Gerand, B., Nowogrocki, G. and Figlarz, M., A new tungsten trioxide hydrate,  $\text{WO}_3 \cdot 1/3\text{H}_2\text{O}$ : preparation, characterization, and crystallographic study. *J. Solid State Chem.*, 1981, **38**, 312–320.
7. Gerand, B., Nowogrocki, G., Guenot, J. and Figlarz, M., Structural study of a new hexagonal form of tungsten trioxide. *M., J. Solid State Chem.*, 1979, **29**, 429–434.
8. Pfeifer, J., Cao, G., Tekula-Buxbaum, P., Kiss, B. A., Farkas-Jahnke, M. and Vadasdi, K., A reinvestigation of the preparation of tungsten oxide hydrate  $\text{WO}_3 \cdot 1/3\text{H}_2\text{O}$ . *J. Solid State Chem.*, 1995, **119**, 90–97.
9. Balázsi, Cs. and Pfeifer, J., Development of tungsten oxyde hydrate phases during precipitation, room temperature ripening and hydrothermal treatment. *Solid State Ionics*, 2002, **151**, 353–358.
10. Balázsi, Cs., Prasad, A. K., Pfeifer, J., Tóth, A. L. and Gouma, P. I., Wet chemical synthesis of nanosize tungsten oxide for sensing applications. In *Proceedings of the First International Workshop on Semiconductor Nanocrystals, SEMINANO 2005, Vol. 1: Materials and Preparation*, ed. B. Pődör, Zs. J. Horváth and P. Basa, 2005, pp. 79–83.
11. Ozkan, E., Lee, S.-Liu, H.P., Tracy, C.E., Tepehan, F.Z., Pitts, J.R. and Deb, S.K., Electrochromic and optical properties of mesoporous tungsten oxide films, *Solid State Ionics*, 2002, **149**, 139–146.
12. Prasad, A.K., Study of gas specificity in  $\text{MoO}_3/\text{WO}_3$  thin film sensors and their arrays, PhD Dissertation, Stony Brook University, Stony Brook NY, USA, May 2005.